Final/Annual/Midterm Report for AOARD Grant AOARD 124016 (12RSZ017)
"**Research Title**" "Understanding of Materials State and its Degradation using Non-Linear Ultrasound (NLU) Approaches-Phase III

Date: 31st May 2013

Name of Principal Investigators (PI and Co-PIs): Krishnan Balasubramaniam
- e-mail address : balas@iitm.ac.in
- Institution : Indian Institute of Technology Madras
- Mailing Address : MDS 301, Department of Mechanical Engineering, IIT Campus, Chennia INDIA 600036
- Phone : +91-44-2257-4662
- Fax : +91-44-2257-0545

Period of Performance: 04/01/2012– 03/31/2013

Abstract: Short summary of most important research results that explain why the work was done, what was accomplished, and how it pushed scientific frontiers or advanced the field. This summary will be used for archival purposes and will be added to a searchable DoD database.

This Phase III research proposal was a continuation effort on the Phase I and II work and the overall program focuses on the development of new explorations towards the development of better understanding of non-linear ultrasonic methods for the quantitative materials state evaluation and characterization of damage in metallic alloys. Both theoretical and experimental works were carried out in order to understand the significance of the effects of microscopic damage in metals using the measurements of Non-Linear Effects of Ultrasound. The Phase III work effort extended the FDTD and the MSLM models t a 2D MSLM model with NLU parameters while solving some of the un-solved problems that were observed in the Phase II. The experimental results were performed on Copper alloys that have damage behavior that can be explained using literature data. The improved understanding of the non-linear ultrasound is anticipated to lead to new measurement techniques that have applications in the area of vehicle health monitoring, nondestructive testing, and process monitoring of manufacturing processes

Introduction:

The work was divided into (a) Theoretical Development using FDTD and MSLM methods and (b) Experimental tasks that develop a relationship between heat treatment of Pure Cu and the Non-Linear Ultrasonic parameters.

Theoretical Development: The details are provided in APPENDIX A.

Experiment: The details are provided in APPENDIX B.

Results and Discussion: The significant results are listed below:
1. FDTD and MSLM models are sufficient to describe materials the homogeneous Non-linear properties in materials.
2. These models have limitations when dealing with dicrete domains and hence an FEM model may be more appropriate for defects that are along grain boundaries in polycrystalline material.
3. Non-Linear ultrasonic measurements can be correlated well with the heat treatment process for both iso-chronic and iso-thermal annealing heat treatement. Sensitivity

Report Documentation Page

Form Approved
OMB No. 0704-0188

1. REPORT DATE	2. REPORT TYPE	3. DATES COVERED
01 MAY 2013	**Final**	**07-03-2012 to 07-02-2013**

4. TITLE AND SUBTITLE
Understanding of Materials State and its Degradation using Non-Linear Ultrasound (NLU) Approaches-Phase III

5a. CONTRACT NUMBER
FA2386-12-1-4016

5b. GRANT NUMBER

5c. PROGRAM ELEMENT NUMBER

6. AUTHOR(S)
Krishnan Balasubramaniam

5d. PROJECT NUMBER

5e. TASK NUMBER

5f. WORK UNIT NUMBER

7. PERFORMING ORGANIZATION NAME(S) AND ADDRESS(ES)
Indian Institute of Technology Madras,MDS 301, Department of Mechanical Engineering, IIT Campus,,Chennia INDIA 600036,Chennia INDIA 600036,IN,600036

8. PERFORMING ORGANIZATION REPORT NUMBER
N/A

9. SPONSORING/MONITORING AGENCY NAME(S) AND ADDRESS(ES)
AOARD, UNIT 45002, APO, AP, 96338-5002

10. SPONSOR/MONITOR'S ACRONYM(S)
AOARD

11. SPONSOR/MONITOR'S REPORT NUMBER(S)
AOARD-124016

12. DISTRIBUTION/AVAILABILITY STATEMENT
Approved for public release; distribution unlimited

13. SUPPLEMENTARY NOTES

14. ABSTRACT

This Phase III research proposal was a continuation effort on the Phase I and II work. The overall program focuses on the development of new explorations towards the development of better understanding of non-linear ultrasonic methods for the quantitative materials state evaluation and characterization of damage in metallic alloys. Both theoretical and experimental works were carried out in order to understand the significance of the effects of microscopic damage in metals using the measurements of Non-Linear Effects of Ultrasound (NLU). The Phase III work effort extended the Finite Difference in Time Domain (FDTD) and the mass-spring lattice models (MSLM) to a 2D MSLM with NLU parameters while resolving some of the issues that were observed in Phase II. The experimental results were performed on copper alloys that have damage behavior that can be explained using literature data. The improved understanding of NLU is anticipated to lead to new measurement techniques that have applications in the area of vehicle health monitoring, nondestructive testing, and process monitoring of manufacturing processes.

15. SUBJECT TERMS
Non-destructive Evaluation Non-linear Ultrasound

16. SECURITY CLASSIFICATION OF:			17. LIMITATION OF ABSTRACT	18. NUMBER OF PAGES	19a. NAME OF RESPONSIBLE PERSON
a. REPORT	b. ABSTRACT	c. THIS PAGE			
unclassified	**unclassified**	**unclassified**	**Same as Report (SAR)**	**37**	

of nonlinear ultrasonic method towards isothermal annealing in pure copper was investigated in this study in great detail.. It was reported that, recovery, recrystallization and grain growth associated with annealing has profound influence on nonlinearity parameter. Presence of precipitates and secondary phase particles, and its effect on nonlinearity parameter was considered by many authors. However, in this study, focus is on the influence of grain-growth on nonlinearity parameter. Variation of non-linearity parameter, β, with different holding durations were analyzed. All the samples were annealed at a temperature above its recrystallization temperature.

4. Further, metallography studies as well as hardness measurements were performed to understand the relationship between microstructural changes and ultrasonic nonlinearity parameter.

List of Publications and Significant Collaborations that resulted from your AOARD supported project: In standard format showing authors, title, journal, issue, pages, and date, for each category list the following:

a) papers published in peer-reviewed journals, NONE
b) papers published in peer-reviewed conference proceedings, NONE
c) papers published in non-peer-reviewed journals and conference proceedings, NONE
d) conference presentations without papers, NONE
e) manuscripts submitted but not yet published, and YES

- R. S. Mini, Krishnan Balasubramaniam, and Parag Ravindran "Nonlinear ultrasonic method for the characterisation of microstructural changes associated with isothermal and isochronous annealing in pure copper", submitted to Acta Materilia (2013)

f) provide a list any interactions with industry or with Air Force Research Laboratory scientists or significant collaborations that resulted from this work. NONE

Attachments: Publications a), b) and c) listed above if possible.

DD882: Attached

APPENDIX A

FDTD and MSLM Model development for studying the Linear and Non-linear ultrasounic interactions with simulated material damage.

Linear and nonlinear wave propagation in a linear elastic isotropic material using Finite Difference in Time Domain(FDTD)

1. Wave propagation through linear isotropic elastic material

A linear elastic material is an ideal case which obeys linear stress-strain relation and can bare only infinitesimally small displacements. Wave equation in 2D can be derived from linearised strain-displacement relation and linear stress-strain relation. The procedure is written below. Equation of motion can be represented in the absence of body forces as

$$\begin{aligned} \rho\frac{\partial^2 u}{\partial t^2} &= \frac{\partial \sigma_{xx}}{\partial x} + \frac{\partial \tau_{xy}}{\partial y} \\ \rho\frac{\partial^2 v}{\partial t^2} &= \frac{\partial \tau_{yx}}{\partial x} + \frac{\partial \sigma_{yy}}{\partial y} \end{aligned} \tag{1}$$

where u,v and w are the x, y and z components of displacement, t is the time, ρ is the density of material σ and τ are the normal and shear stress components respectively. The linearised strain-displacement can be written as

$$\epsilon_{ij} = \frac{1}{2}\left[\frac{\partial u_i}{\partial x_k} + \frac{\partial u_k}{\partial x_i}\right] \tag{2}$$

where ϵ_{ij} is the strain tensor. For a linear elastic isotropic material constitutive equation can be written

$$\sigma_{ij} = 2\mu\epsilon_{ij} + \lambda \mathbf{tr}(\epsilon_{ij})\,\delta_{kk} \tag{3}$$

where λ and μ are the Lame's constant and δ_{kk} is the Kronecker delta. On substituting eqn. (2) and eqn. (3) in eqn (1) we get the wave equation. The

wave equation in 2D thus obtained is

$$\rho\frac{\partial^2 u}{\partial t^2} = (\lambda+2\mu)\frac{\partial^2 u}{\partial x^2} + (\lambda+\mu)\frac{\partial v}{\partial x\partial y} + \mu\frac{\partial^2 u}{\partial y^2}$$
$$\rho\frac{\partial^2 v}{\partial t^2} = (\lambda+2\mu)\frac{\partial^2 v}{\partial y^2} + (\lambda+\mu)\frac{\partial u}{\partial x\partial y} + \mu\frac{\partial^2 v}{\partial x^2} \tag{4}$$

2. Initial condition and Boundary condition

Velocity and displacement are considered as zero initially. Rigid and free surface boundary conditions were considered in the present study.

2.1. Initial condition

When time $t = 0$, displacement and velocity components are zero.
ie.

$$u = v = 0$$
$$\frac{\partial u}{\partial t} = \frac{\partial v}{\partial t} = 0 \tag{5}$$

2.2. Boundary condition

Displacement components are zero when boundaries are considered as rigid. ie

$$u = 0$$
$$v = 0 \tag{6}$$

Stress free boundary is otherwise known as free surface condition. On the free surface, normal and shear components of stress are zero. In this study x axis is considered as pointing vertically downwards and y axis is parallel to the horizontal free surface. Both vertical and horizontal surfaces are assumed to be free. ie

$$\sigma_x = \sigma_y = \tau_{xy} = \tau_{yx} = 0$$

Hence for horizontal free surface

$$(\lambda+2\mu)\frac{\partial u}{\partial x} + \lambda\frac{\partial v}{\partial y} = 0$$
$$\mu\left[\frac{\partial u}{\partial y} + \frac{\partial v}{\partial x}\right] = 0. \tag{7}$$

and for vertical free surface

$$(\lambda + 2\mu)\frac{\partial v}{\partial y} + \lambda\frac{\partial u}{\partial x} = 0$$
$$\mu\left[\frac{\partial u}{\partial y} + \frac{\partial v}{\partial x}\right] = 0. \tag{8}$$

3. Problem solving-Numerical approach

Wave propagation problem in the present case is solved using Finite Difference in Time Domain (FDTD) which uses Finite Difference Method. FDTD proved itself as an important tool for investigating elasto-dynamic problems. It is a grid point method in which the values of the field quantities are defined only on the nodal points. As the equation is solved in time domain it known as FDTD. A rectangular grid with dx and dy as the increments in space is superimposed on the domain. Discretisation with respect to time is done with an increment of dt. For simplicity and convenience, it is assumed that space step, $dx = dy = h$. The wave equation which is a PDE is converted to its corresponding difference form using forward, backward or central difference method. Along with the boundary conditions and initial conditions, obtained difference equation is solved using any of the explicit or implicit method.

4. Simulation of wave propagation through linear elastic material-1D

For one dimensional wave, eqn. (4) can be written as

$$\rho\frac{\partial^2 u}{\partial t^2} = (\lambda + 2\mu)\frac{\partial^2 u}{\partial x^2} \tag{9}$$

and its finite difference equation using centre-difference method can be expressed as

$$\rho\left[\frac{u_{i,j+1} - 2u_{i,j} + u_{i,j-1}}{dt^2}\right] = (\lambda + 2\mu)\left[\frac{u_{i+1,j} - 2u_{i,j} + u_{i-1,j}}{h^2}\right]. \tag{10}$$

Let $u_{i,j}$ be the displacement at the i^{th} node at j^{th} time step. Displacement for the next time step $(j+1)$, can be obtained from the known values of previous time steps (j) and $(j-1)$. This approach is known as explicit method. Hence

Table 1: Parameters used in numerical simulation

Material	Steel
Young's modulus	200 MPa
Density	$7800 kg/m^3$
Poisson's ratio	0.3
Length	0.5 m
Frequency	0.1 MHz

displacement for $(j+1)^{th}$ time step can be determined using the following equation.

$$u_{i,j+1} = 2u_{i,j} - u_{i,j-1} + \frac{dt^2}{h^2}\frac{(\lambda + 2\mu)}{\rho}\left[u_{i+1,j} - 2u_{i,j} + u_{i-1,j}\right] \tag{11}$$

A MATLAB code was written for finding the displacement at each node for all time steps. Material selected for the study was steel with 1 m length. A 5 cycle tone burst signal with 0.1MHz frequency was used in the simulation. Various parameters used for the simulation are given in Table.1. Element size chosen was $\frac{1}{32}$ of a wavelength to prevent spatial aliasing and time step was selected based on the Courant Friedrichs Lewy (CFL) condition, $\frac{Cdt}{dx} \leq 1$. Here in this study, time step

$$dt = \frac{h}{\sqrt{2}C_l}, \tag{12}$$

where C_l is the longitudinal velocity. Time domain signal thus obtained and its corresponding fast fourier transform is given in Fig. 1 (a) and (b) respectively. Simulation was done separately with rigid and free surface condition. Phase change of the signal occurs when it reaches rigid boundary whereas it is not happening in the case of free surface condition. Difference in the signal observed with those conditions are given in fig in 2(a) and (b)respectively.

5. Simulation of wave propagation through linear elastic material-2D

In 2D, three types of problems were considered.

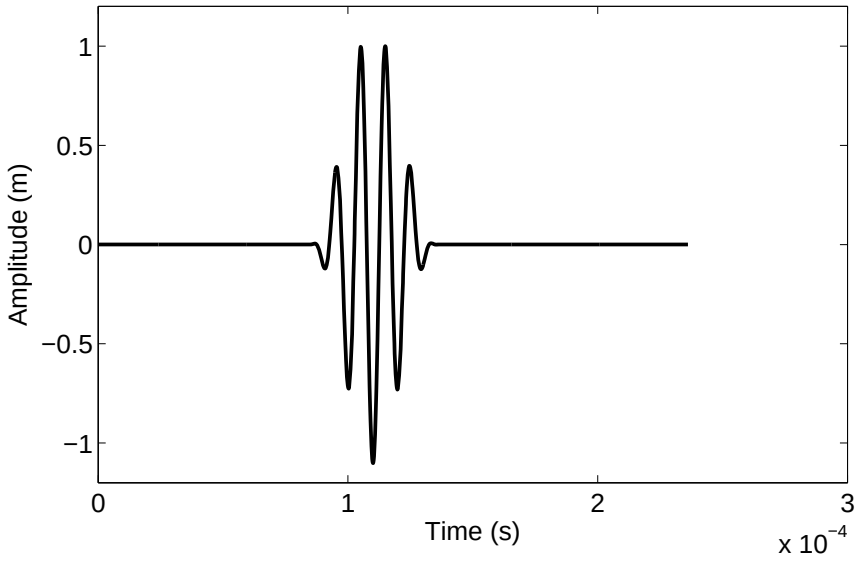

(a)

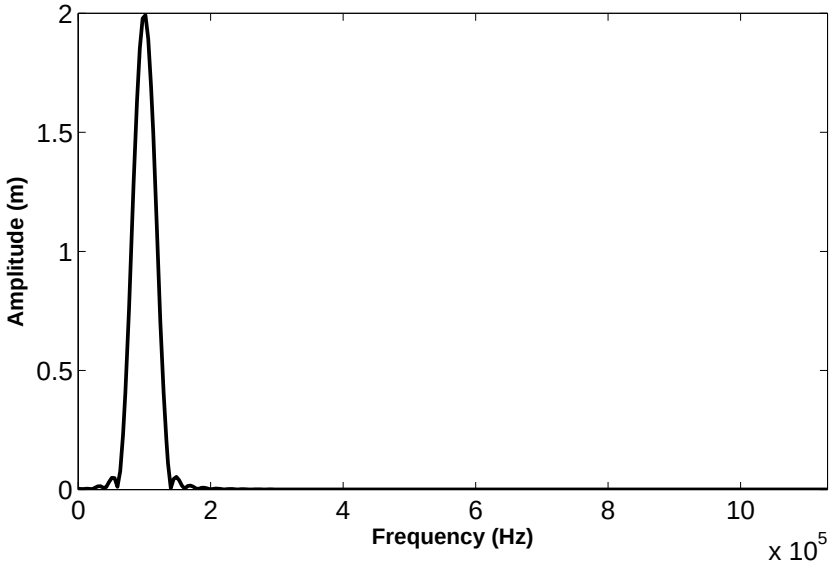

(b)

Figure 1: (a)Time domain signal obtained for linear wave propagation simulation in 1D (b) FFT obtained for linear wave propagation simulation in 1D

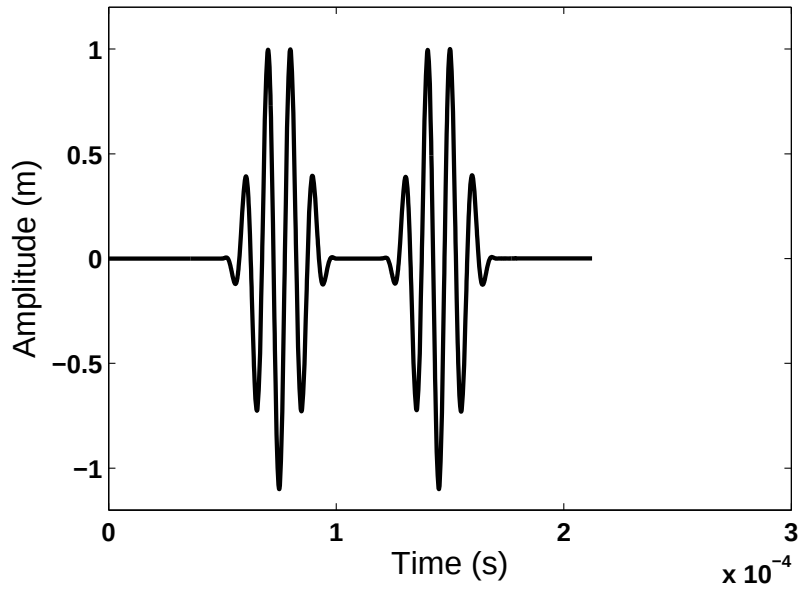

(a)

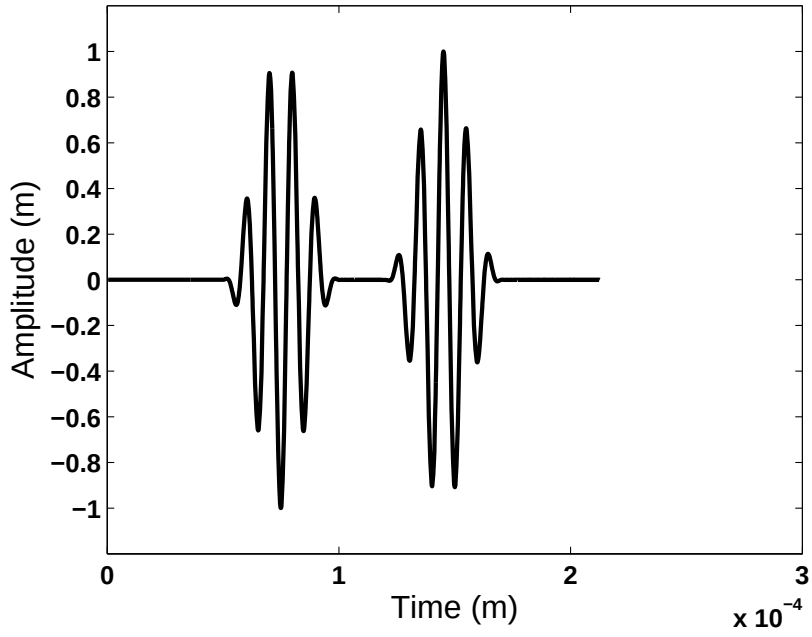

(b)

Figure 2: (a)Simulation for free surface boundary condition (b) Simulation for rigid boundary condition

Table 2: Parameters used in numerical simulation

Material	Steel
Young's modulus	200 MPa
Density	$7800 kg/m^3$
Poisson's ratio	0.3
Length	0.5 m
breadth	0.5 m
Frequency	0.1 MHz

- Wave propagation in a bulk material.
- Wave propagation in an elastic half space.
- Wave propagation in a plate.

5.1. Wave propagation in a bulk material-Bulk wave

Let us consider the simulation of wave propagation in a 2D domain. Dimensions of the domain and other parameters used for the simulation are given in Table 2. Schematic of the domain used in the simulation is given in Fig. 3(a). Displacement components obtained from the finite difference form of eqn. 4 for all time-steps can be written as

$$u_{i,j,k+1} = 2u_{i,j,k} - u_{i,j,k-1} + \frac{dt^2}{h^2}(\lambda + 2\mu)\left[u_{i+1,j,k} - 2u_{i,j,k} + u_{i-1,j,k}\right] + \frac{dt^2}{4h^2}(\lambda + \mu)$$
$$\left[v_{i+1,j+1,k} - v_{i+1,j-1,k} - v_{i-1,j+1,k} + v_{i-1,j-1,k}\right] + \frac{dt^2}{h^2}\mu\left[u_{i,j+1,k} - 2u_{i,j,k} + u_{i,j-1,k}\right]$$
$$v_{i,j,k+1} = 2v_{i,j,k} - v_{i,j,k-1} + \frac{dt^2}{h^2}(\lambda + 2\mu)\left[v_{i,j+1,k} - 2v_{i,j,k} + v_{i,j-1,k}\right] + \frac{dt^2}{4h^2}(\lambda + \mu)$$
$$\left[u_{i+1,j+1,k} - u_{i+1,j-1,k} - u_{i-1,j+1,k} + u_{i-1,j-1,k}\right] + \frac{dt^2}{h^2}\mu\left[v_{i+1,j,k} - 2v_{i,j,k} + u_{i-1,j,k}\right]. \quad (13)$$

Result obtained when the excitation was given at the centre of the domain is given in Fig. 3(b). Longitudinal waves are seen in the direction of excitation and shear waves propagate perpendicular to it. As the boundaries are at infinity, it is not required to specify any boundary condition in this case.

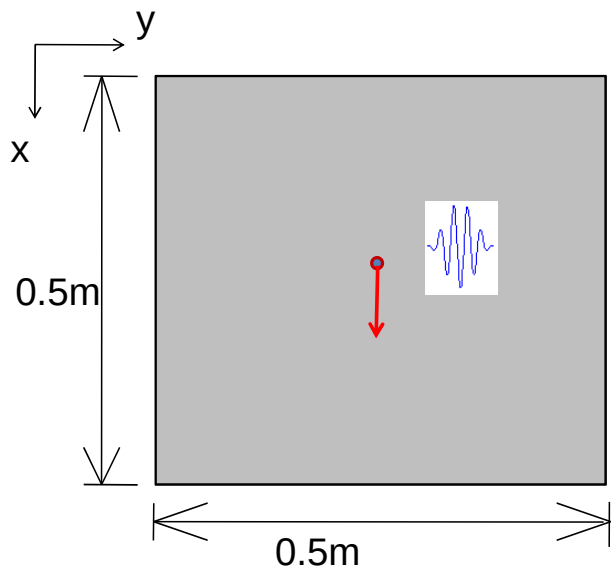

(a)

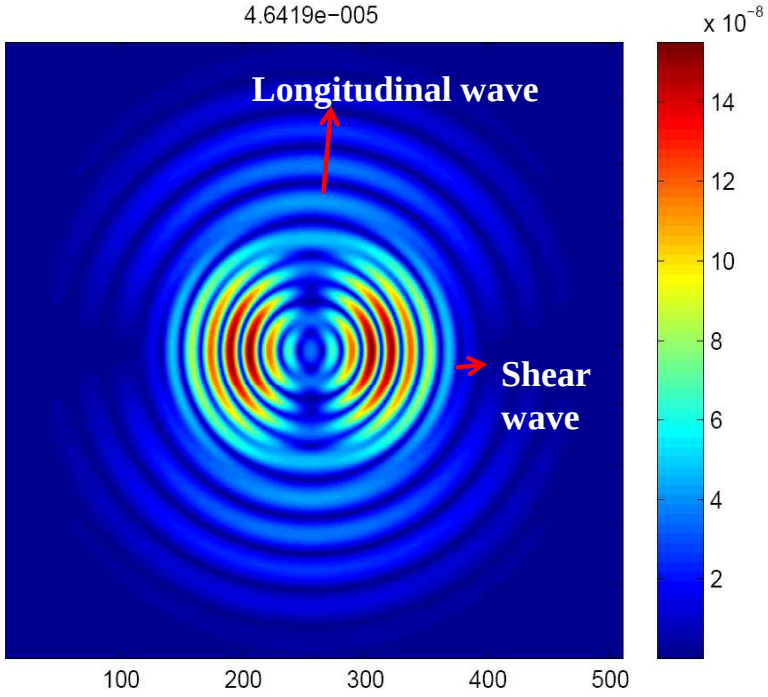

(b)

Figure 3: (a)Domain used for wave propagation in a bulk material. (b) Result obtained from wave propagation simulation.

5.2. Wave propagation in an elastic half space-Rayleigh wave

Elastic half-space is a domain in which free surface boundary condition is applicable in at least one surface and other boundaries are assumed to be at infinity. The domain selected for wave propagation in an elastic half space is given in Fig. 4(a).

Implementation of free surface boundary condition is one of the most delicate and difficult task in wave propagation problems. Normal and shear stress vanishes on those surfaces where free surface or stress free boundary is assumed. New Composed method developed by Ilan, was used for the implementation of this boundary condition. In this method, displacement of fictitious points are not required for finding the displacement at free surface. The Taylor series expansion of the vertical component of displacement around a surface point can be written as

$$u_{2,j,k} = u_{1,j,k} + h\frac{\partial u_{1,j,k}}{dx} + \frac{h^2}{2}\frac{\partial^2 u_{1,j,k}}{dx^2} + O(dx^3) \tag{14}$$

On substituting $\frac{\partial u}{\partial x}$ and $\frac{\partial^2 u}{\partial x^2}$ obtained from the boundary condition (eqn. 7) and wave equation (eqn. 4) in eqn. (15), displacement of nodes at the free surface for all the time steps can be determined. It can be written as

$$\begin{aligned} u_{1,j,k+1} = 2u_{i,j,k} - u_{i,j,k-1} + 2\frac{(\lambda+2\mu)}{\rho}\frac{dt^2}{h^2}\left[u_{2,j,k} - u_{i,j,k}\right] + \frac{\lambda}{h^2\rho}\left[v_{i,j+1,k} - v_{i,j-1,k}\right] \\ + \frac{(\lambda+\mu)dt^2}{4h^2\rho}\left[v_{i+1,j+1} - v_{i+1,j-1,k} - v_{i-1,j+1,k} + v_{i-1,j-1,k}\right] \\ + \frac{\mu dt^2}{\rho h^2}\left[u_{i,j+1,k} - 2u_{i,j,k} + u_{i,j-1,k}\right]. \end{aligned} \tag{15}$$

The same procedure can be used for the determination of horizontal component of displacement. A five cycle tone burst with 100 kHz frequency is applied on the top surface. The simulation thus obtained is shown in Fig. 4(b). Apart from the bulk waves, rayleigh waves are also seen in the simulation. Head waves connecting longitudinal and shear waves are also visible in Fig. 4(b). The time domain signal obtained for a node on the free surface and its corresponding fft is given in Fig. 5(a) and (b)respectively.

5.3. Wave propagation in a plate-Lamb waves

Governing equation for a plate wave is also same as that for a bulk wave. Free surface condition has to be incorporated on both surfaces (top and

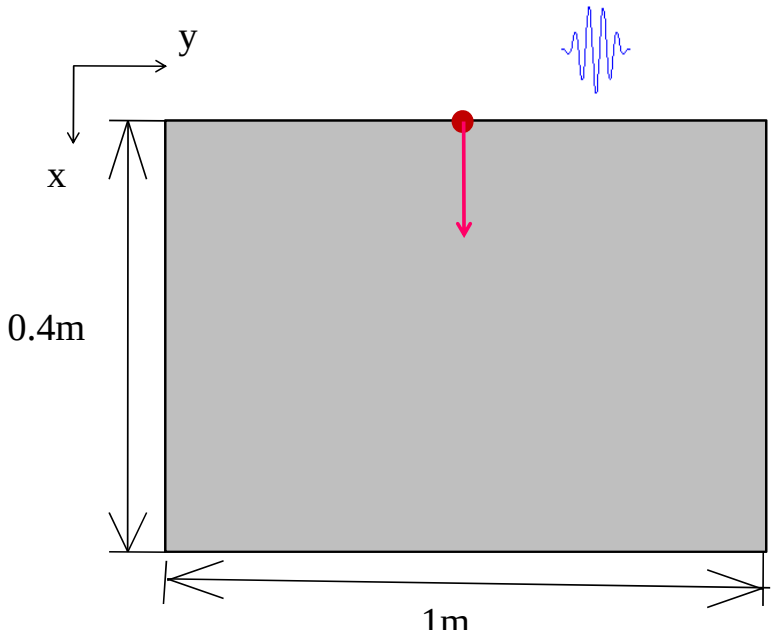

(a)

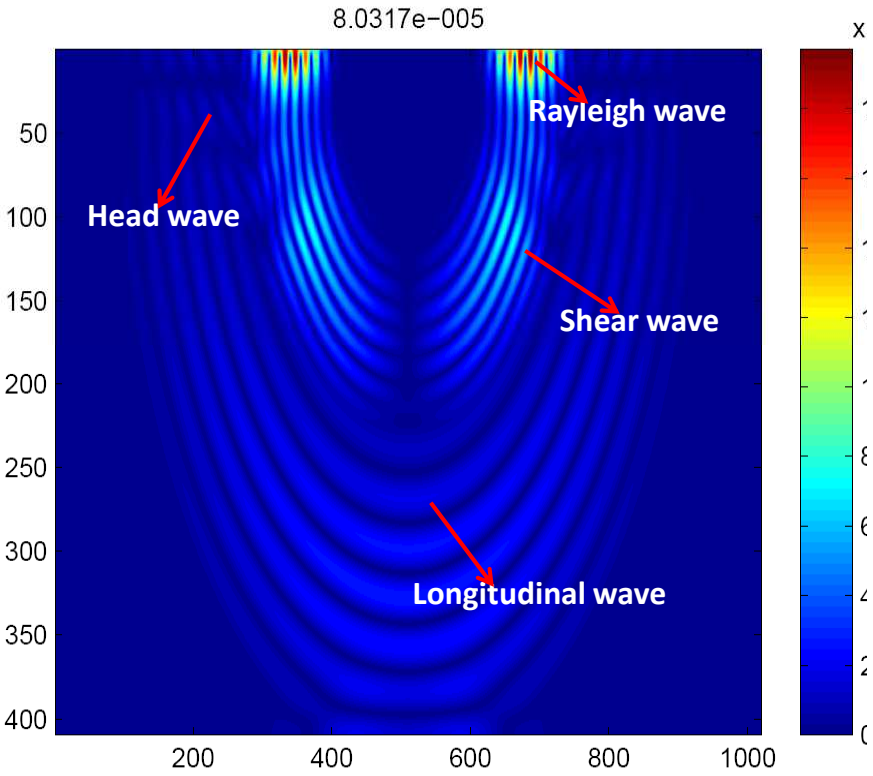

(b)

Figure 4: (a)Domain considered for wave propagation in elastic half space.(b) Result obtained for the wave propagation simulation.

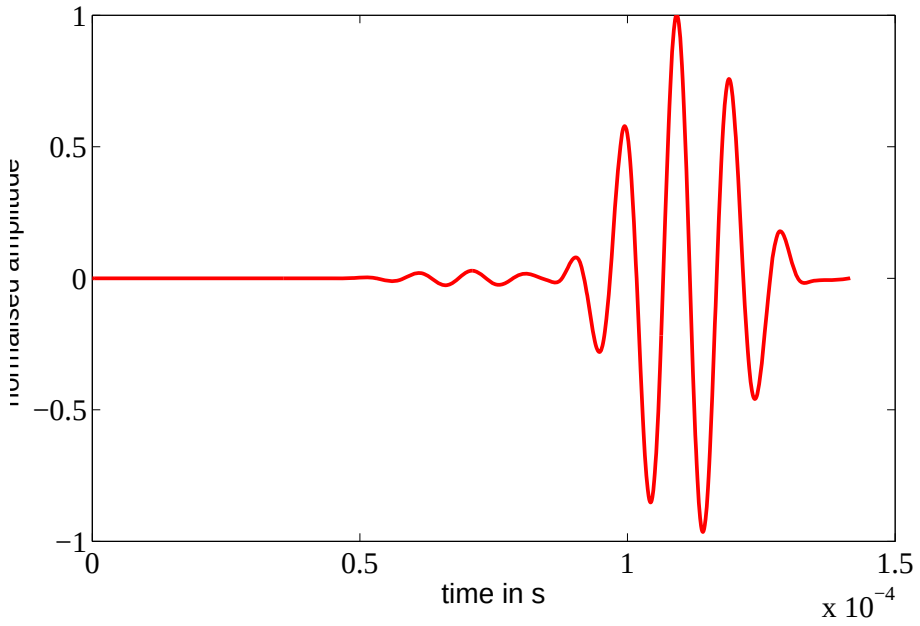

(a)

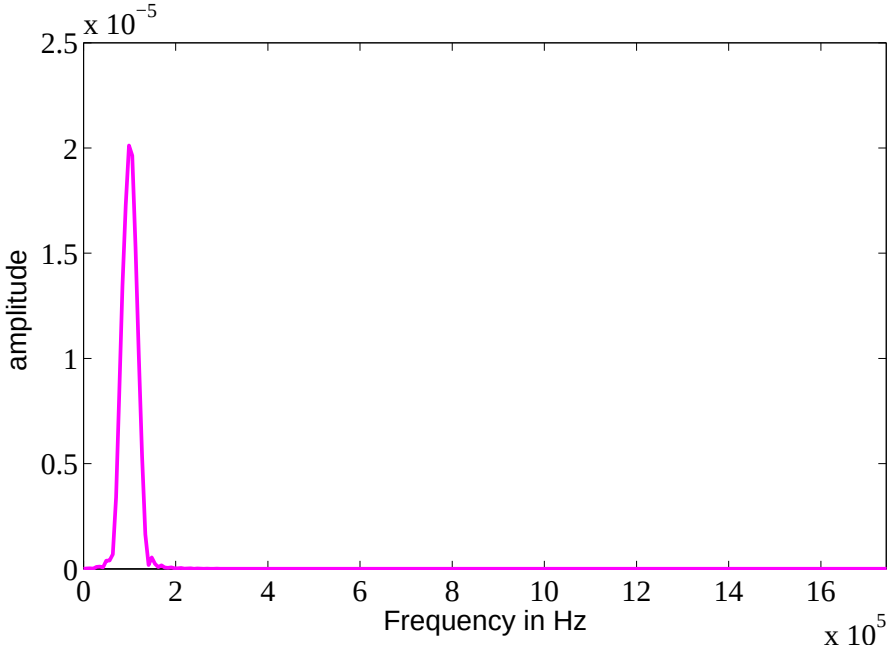

(b)

Figure 5: (a)Time domain signal of a node on the free surface.(b)FFT of the corresponding signal.

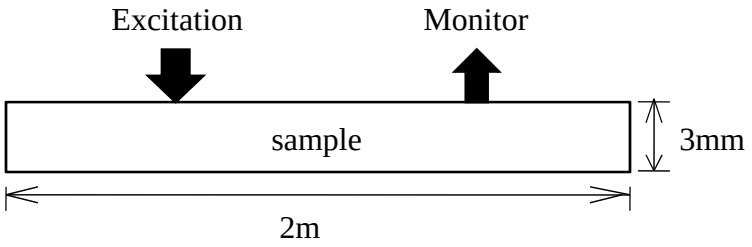

Figure 6: Schematic of the domain used for the simulation of lamb wave

bottom) of the domain (thin plate) considered for the numerical simulation. Schematic of the domain considered for the numerical simulation with the direction of excitation is given in Fig. 6. Excitation was given at 10 nodes on the top surface at $\frac{1}{3}$ distance from the left edge. Results obtained for the simulation at different instants is given in Fig. 7. Signals corresponding to the vertical and horizontal displacement obtained at a node which is $\frac{1}{3}$ distance from the right end is given in Fig.8. Results obtained for lamb wave propagation when the excitation was given in the horizontal direction is given in Fig. 9. Vertical and horizontal displacements obtained for that is given in Fig. 10

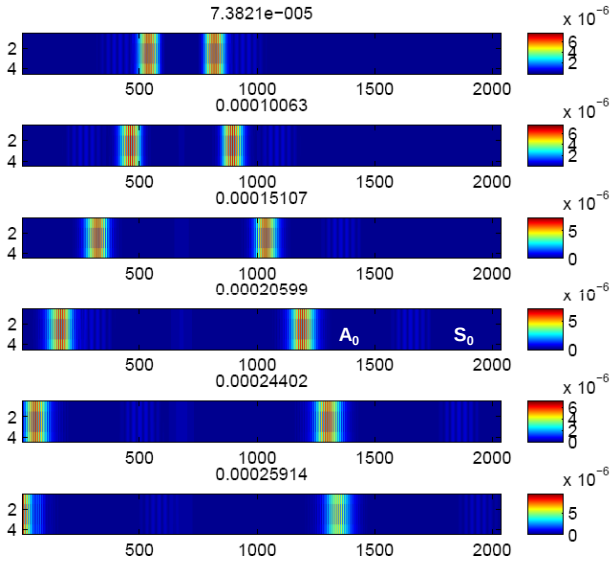

Figure 7: Lamb wave at different time instants when vertical excitation was given

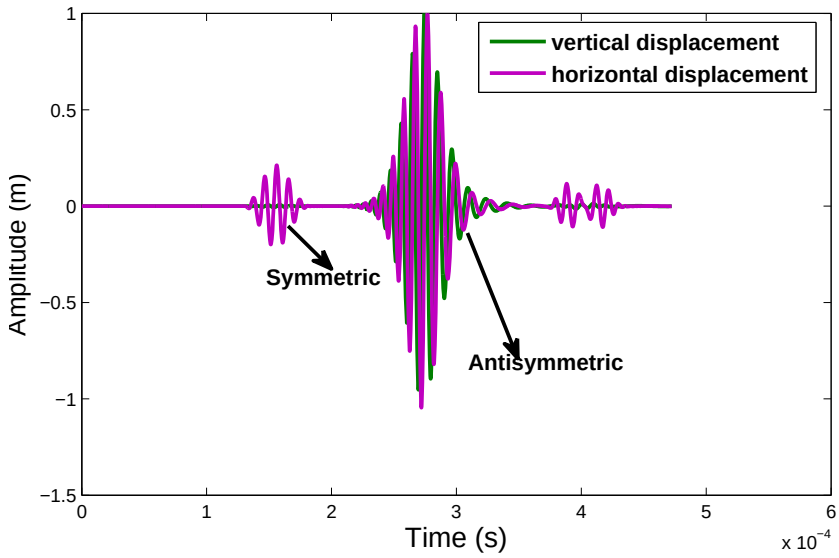

Figure 8: Vertical and horizontal displacement obtained when the excitation was given in the vertical direction

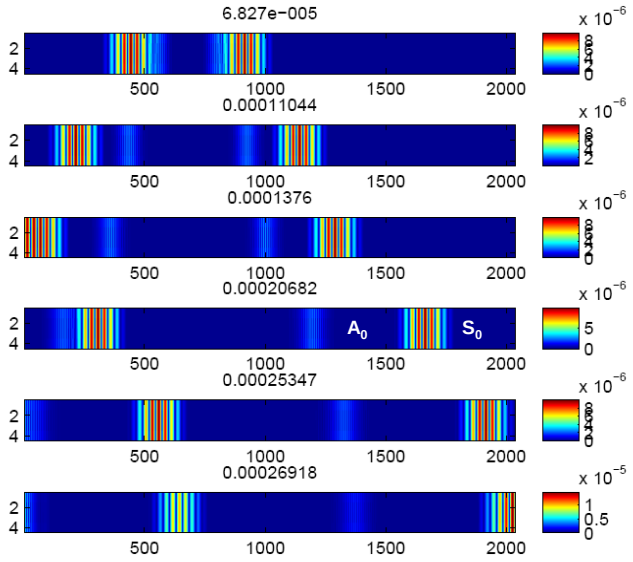

Figure 9: Lamb wave at different time instants when horizontal excitation was given

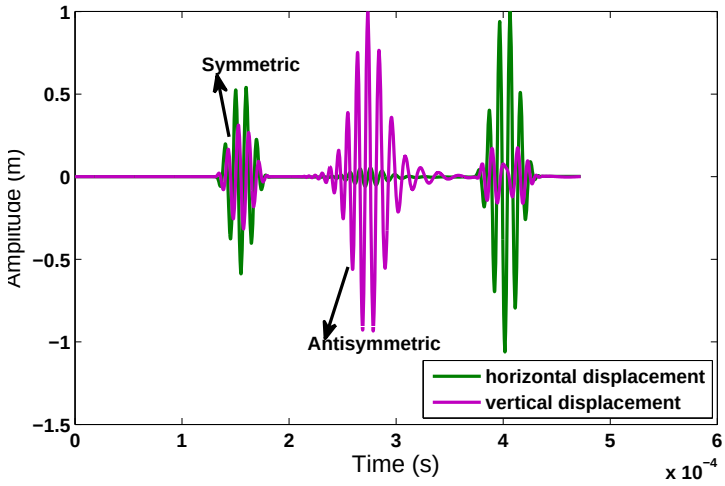

Figure 10: Signals of Vertical and horizontal displacements when excitation was given in the vertical direction

6. Non-linear Wave Equation

Nonlinearities can be broadly classified into material nonlinearity and geometric nonlinearity. Material nonlinearity is one in which the stress-strain relation is nonlinear whereas the strain-displacement relation is nonlinear in geometric nonlinearity. Mixed nonlinearity is one in which both stress-strain relation and strain-displacement relation are nonlinear. Nonlinearity due to geometric nonlinearity alone is considered in this work. Material considered is linear elastic and isotropic. The procedure adopted for the derivation of wave equation is given below. The Cauchy green strain-displacement relation in its complete form can represented as

$$\epsilon_{ij} = \frac{1}{2}\left[\frac{\partial u_i}{\partial x_k} + \frac{\partial u_k}{\partial x_i} + \frac{\partial u_l}{\partial x_k}\frac{\partial u_l}{\partial x_i}\right]. \tag{16}$$

Constitutive equation used was the stress-strain relation for a homogeneous, linear elastic isotropic material. The stress components obtained by substituting eqn. (16) in the constitutive equation is written as

$$\begin{aligned}
\sigma_{xx} &= \frac{\lambda+2\mu}{2}\left[2\frac{\partial u}{\partial x} + \left(\frac{\partial u}{\partial x}\right)^2 + \left(\frac{\partial v}{\partial x}\right)^2\right] + \frac{\lambda}{2}\left[2\frac{\partial v}{\partial y} + \left(\frac{\partial u}{\partial y}\right)^2 + \left(\frac{\partial v}{\partial y}\right)^2\right], \\
\sigma_{yy} &= \frac{\lambda+2\mu}{2}\left[2\frac{\partial v}{\partial y} + \left(\frac{\partial u}{\partial y}\right)^2 + \left(\frac{\partial v}{\partial y}\right)^2\right] + \frac{\lambda}{2}\left[2\frac{\partial u}{\partial x} + \left(\frac{\partial u}{\partial x}\right)^2 + \left(\frac{\partial v}{\partial x}\right)^2\right] \\
\tau_{xy} &= \tau_{yx} = \mu\left[\frac{\partial u}{\partial y} + \frac{\partial v}{\partial x} + \frac{\partial u}{\partial x}\frac{\partial u}{\partial y} + \frac{\partial v}{\partial v}\frac{\partial v}{\partial y}\right]
\end{aligned} \tag{17}$$

On substituting the stress components in the equation of motion (eqn. 1) yields the nonlinear wave equation as

$$\begin{aligned}
\rho\frac{\partial^2 u}{\partial t^2} &= (\lambda+2\mu)\left[\frac{\partial^2 u}{\partial x^2} + \frac{\partial u}{\partial x}\frac{\partial^2 u}{\partial x^2} + \frac{\partial v}{\partial x}\frac{\partial^2 v}{\partial x^2}\right] + (\lambda+\mu)\left[\frac{\partial^2 v}{\partial x \partial y} + \frac{\partial u}{\partial y}\frac{\partial^2 u}{\partial x \partial y} + \frac{\partial v}{\partial y}\frac{\partial^2 v}{\partial x \partial y}\right] \\
&\quad +\mu\left[\frac{\partial^2 u}{\partial y^2} + \frac{\partial u}{\partial x}\frac{\partial^2 u}{\partial y^2} + \frac{\partial v}{\partial x}\frac{\partial^2 v}{\partial y^2}\right] \\
\rho\frac{\partial^2 v}{\partial t^2} &= (\lambda+2\mu)\left[\frac{\partial^2 v}{\partial y^2} + \frac{\partial u}{\partial y}\frac{\partial^2 u}{\partial y^2} + \frac{\partial v}{\partial y}\frac{\partial^2 v}{\partial y^2}\right] + (\lambda+\mu)\left[\frac{\partial^2 u}{\partial x \partial y} + \frac{\partial u}{\partial x}\frac{\partial^2 u}{\partial x \partial y} + \frac{\partial v}{\partial x}\frac{\partial^2 v}{\partial x \partial y}\right] \\
&\quad +\mu\left[\frac{\partial^2 v}{\partial x^2} + \frac{\partial u}{\partial y}\frac{\partial^2 u}{\partial x^2} + \frac{\partial v}{\partial y}\frac{\partial^2 v}{\partial x^2}\right]
\end{aligned} \tag{18}$$

6.1. Initial conditions and Boundary conditions

Displacement and velocity were considered as zero in the initial condition. As in the linear wave simulation, two types of boundary condition were considered for this study. Displacement components are zero for a rigid boundary. In the free surface or traction free surface, normal and shear stress components are zero. Thus

$$\sigma_{xx} = \lambda + 2\mu \left[2\frac{\partial u}{\partial x} + \left(\frac{\partial u}{\partial x}\right)^2 + \left(\frac{\partial v}{\partial x}\right)^2 \right] + \lambda \left[2\frac{\partial v}{\partial y} + \left(\frac{\partial u}{\partial y}\right)^2 + \left(\frac{\partial v}{\partial y}\right)^2 \right] = 0 \tag{19}$$

$$\sigma_{yy} = \frac{\lambda + 2\mu}{2} \left[2\frac{\partial v}{\partial y} + \left(\frac{\partial u}{\partial y}\right)^2 + \left(\frac{\partial v}{\partial y}\right)^2 \right] + \frac{\lambda}{2} \left[2\frac{\partial u}{\partial x} + \left(\frac{\partial u}{\partial x}\right)^2 + \left(\frac{\partial v}{\partial x}\right)^2 \right] = 0 \tag{20}$$

$$\tau_{xy} = \mu \left[\frac{\partial u}{\partial y} + \frac{\partial v}{\partial x} + \frac{\partial u}{\partial x}\frac{\partial u}{\partial y} + \frac{\partial v}{\partial v}\frac{\partial v}{\partial y} \right] = 0. \tag{21}$$

7. Numerical simulation of nonlinear wave propagation using FDTD-1D

Nonlinear wave equation in one dimension can be written as

$$\rho \frac{\partial^2 u}{\partial t^2} = (\lambda + 2\mu) \left[\frac{\partial^2 u}{\partial x^2} + \frac{\partial u}{\partial x}\frac{\partial^2 u}{\partial x^2} \right] \tag{22}$$

7.1. Numerical Modelling

The partial derivatives in the governing equations are discretised using central difference method and it can be applied for the interior points of the domain. Displacement of the i^{th} node, obtained from the finite difference equation, for all time steps can be written as

$$\begin{aligned} u_{i,j+1} = 2u_{i,j} - u_{i,j-1} + \frac{dt^2}{h^2}\frac{(\lambda + 2\mu)}{\rho}(u_{i+1,j} - 2u_{i,j} + u_{i-1,j}) + \\ \frac{dt^2}{h^2}\frac{(\lambda + 2\mu)}{\rho}(u_{i+1,j} - 2u_{i,j} + u_{i-1,j})(u_{i+1,j} - u_{i-1,j}) \end{aligned} \tag{23}$$

Domain considered for the simulation is same as that for linear 1D case. Time domain signal obtained for the end node when free surface boundary condition is applied is given in Fig.11.

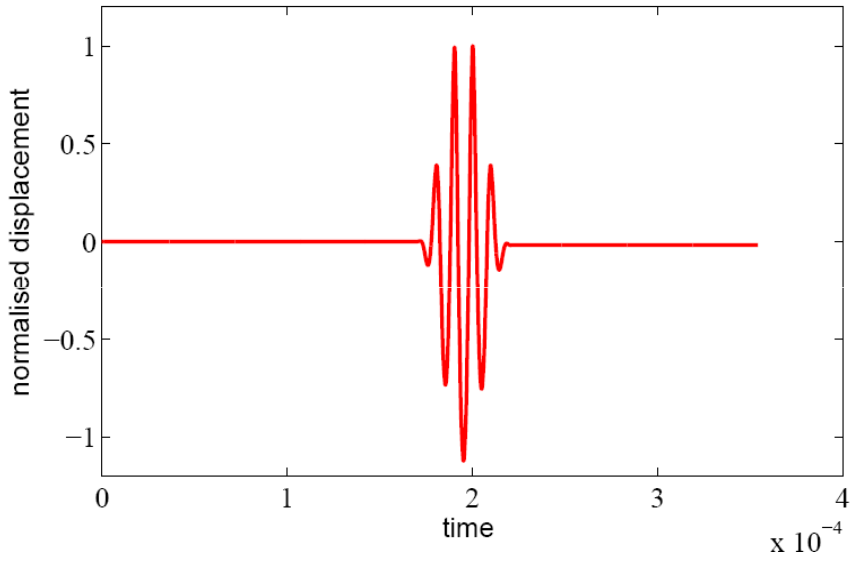

(a)

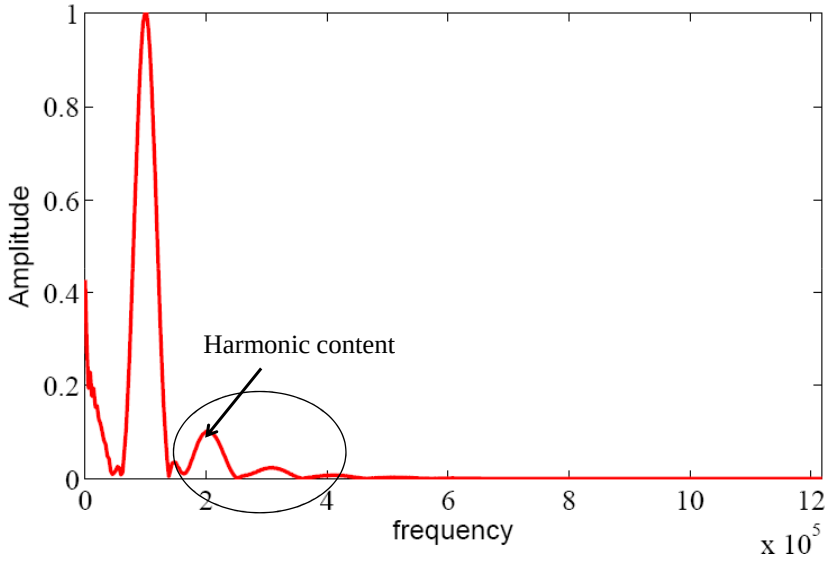

(b)

Figure 11: (a)Time domain signal obtained for nonlinear wave propagation simulation in 1D (b) FFT obtained for nonlinear wave propagation simulation in 1D

8. Numerical simulation of nonlinear wave propagation using FDTD-2D

The discretisation of 2D nonlinear wave equation yields the displacements as

$$u_{i,j}^{k+1} = 2u_{i,j}^{k} + u_{i,j}^{k-1} + \frac{(\lambda+2\mu)}{\rho}\frac{dt^2}{h^2}\left[u_{i+1,j}^{k} - 2u_{i,j}^{k} + u_{i-1,j}^{k}\right] + \frac{(\lambda+2\mu)}{\rho}\frac{dt^2}{2h^3}$$
$$\left[\left(u_{i+1,j}^{k} - u_{i-1,j}^{k}\right)\left(u_{i+1,j}^{k} - 2u_{i,j}^{k} + u_{i-1,j}^{k}\right) + \left(v_{i+1,j}^{k} - v_{i-1,j}^{k}\right)\left(v_{i+1,j}^{k} - 2v_{i,j}^{k} + v_{i-1,j}^{k}\right)\right]$$

$$+\left[\frac{\lambda+\mu}{\rho}\frac{dt^2}{4h^2}\right]\left(v_{i+1,j+1}^{k} - v_{i-1,j+1}^{k} - v_{i+1,j-1}^{k} + v_{i-1,j-1}^{k}\right) + \left[\frac{(\lambda+\mu)}{\rho}\frac{dt^2}{8h^3}\right]$$
$$\left[\left(u_{i,j+1}^{k} - u_{i,j-1}^{k}\right)\left(u_{i+1,j+1}^{k} - u_{i+1,j-1}^{k} - u_{i-1,j+1}^{k} + u_{i-1,j-1}^{k}\right)\right.$$
$$\left.+\left(v_{i,j+1}^{k} - v_{i,j-1}^{k}\right)\left(v_{i+1,j+1}^{k} - v_{i-1,j+1}^{k} - v_{i+1,j-1}^{k} + v_{i-1,j-1}^{k}\right)+\frac{\mu}{\rho}\frac{dt^2}{h^2}\left(u_{i,j+1}^{k} - 2u_{i,j}^{k} + u_{i,j-1}^{k}\right)\right.$$
$$\left.+\left[\frac{\mu}{\rho}\frac{dt^2}{2h^3}\right]\left[\left(u_{i+1,j}^{k} - u_{i-1,j}^{k}\right)\left(u_{i,j+1}^{k} - 2u_{i,j}^{k} + u_{i,j-1}^{k}\right)\left(v_{i+1,j}^{k} - v_{i-1,j}^{k}\right)\left(v_{i,j+1}^{k} - 2v_{i,j}^{k} + v_{i,j-1}^{k}\right)\right]\right. \quad (24)$$

$$v_{i,j}^{k+1} = 2v_{i,j}^{k} + v_{i,j}^{k-1} + \frac{(\lambda+2\mu)}{\rho}\frac{dt^2}{h^2}\left(v_{i,j+1}^{k} - 2v_{i,j}^{k} + v_{i,j-1}^{k}\right) + \frac{(\lambda+2\mu)}{\rho}\frac{dt^2}{2h^3}$$

$$\left[\left(u_{i,j+1}^{k} - u_{i,j-1}^{k}\right)\left(u_{i,j+1}^{k} - 2u_{i,j}^{k} + u_{i,j-1}^{k}\right) + \left(v_{i,j+1}^{k} - v_{i,j-1}^{k}\right)\left(v_{i,j+1}^{k} - 2v_{i,j}^{k} + v_{i,j-1}^{k}\right)\right]$$
$$+\left[\frac{(\lambda+\mu)}{\rho}\frac{dt^2}{4h^2}\right]\left(u_{i+1,j+1}^{k} - u_{i-1,j+1}^{k} - u_{i+1,j-1}^{k} + u_{i-1,j-1}^{k}\right) + \frac{(\lambda+\mu)}{\rho}\frac{dt^2}{8h^3}$$
$$\left[\left(u_{i+1,j}^{k} - u_{i-1,j}^{k}\right)\left(u_{i+1,j+1}^{k} - u_{i+1,j-1}^{k} - u_{i-1,j-1}^{k} + u_{i-1,j-1}^{k}\right)\right.$$
$$\left.+(\mathrm{v}_{i+1,j}^{k} - v_{i-1,j}^{k}\left(v_{i+1,j+1}^{k} - v_{i-1,j+1}^{k} - v_{i+1,j-1}^{k} + v_{i-1,j-1}^{k}\right)\right]+\left[\frac{\mu}{\rho}\frac{dt^2}{h^2}\right]\left(v_{i+1,j}^{k} - 2v_{i,j}^{k} + v_{i-1,j}^{k}\right)$$
$$\left.+\left[\frac{\mu}{\rho}\frac{dt^2}{2h^3}\right]\left[\left(u_{i,j+1}^{k} - u_{i,j-1}^{k}\right)\left(u_{i+1,j}^{k} - 2u_{i,j}^{k} + u_{i-1,j}^{k}\right) + \left(v_{i,j+1}^{k} - v_{i,j-1}^{k}\right)\left(v_{i+1,j}^{k} - 2v_{i,j}^{k} + v_{i-1,j}^{k}\right)\right]\right. \quad (25)$$

The above difference equation can be used for the entire domain except the boundary. Ghost point method is used for finding the displacement components of nodes on the boundary. The dimensions of the domain considered for the present study is same as that for the linear wave simulation.

8.1. Nonlinear wave propagation in the bulk of a material

There is no need to specify any specific boundary condition for the wave propagation in the bulk of the material. The result obtained obtained is depicted in Fig. 12(a). Longitudinal and shear waves are seen in the simulated wave. Simulated wave and time domain signal looks almost similar to that of linear wave, but the fast Fourier transform contain harmonic contents. FFT of such a time domain signal is given in Fig.12(b).

8.2. Nonlinear wave propagation in an elastic half space-Nonlinear Rayleigh wave

New composed method introduced by Ilan found to be suitable for a large number of linear elastic materials to tackle free surface boundary condition. It does not require fictitious layer and found to be stable. For nonlinear Rayleigh wave simulation, a method which is similar to fictitious or ghost point method is used for the implementation of boundary condition. From the boundary condition for zero shear stress, (eqn. 21), $\frac{\partial v}{\partial x}$ is determined and on substituting that in the eqn. 19 yields a quadratic equation in $\frac{\partial u}{\partial x}$. From the difference equations of $\frac{\partial u}{\partial x}$ and $\frac{\partial v}{\partial x}$, displacements of the free surface can be determined. Results obtained when the excitation was given at the centre of the top surface, at different time periods is given in Fig.13. A time domain signal obtained for a node on the top surface and its corresponding fft is given in Fig.14.

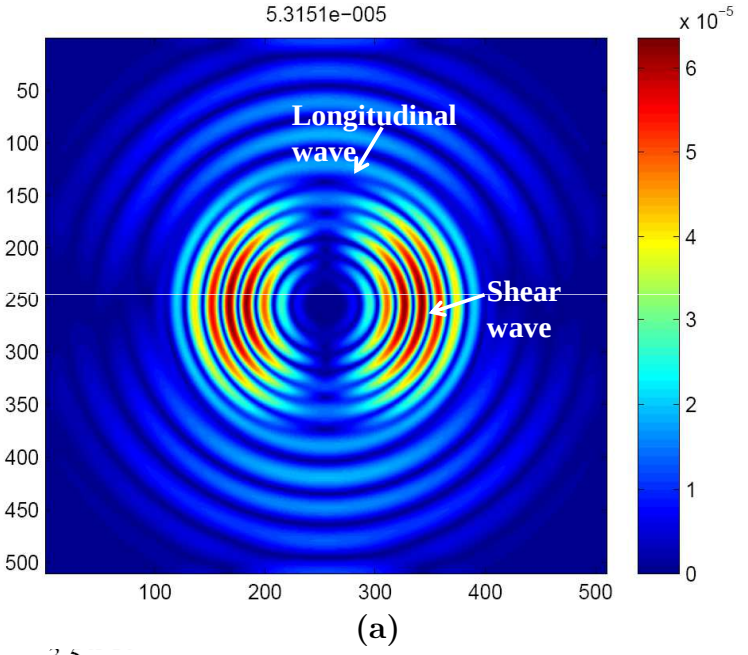

(a)

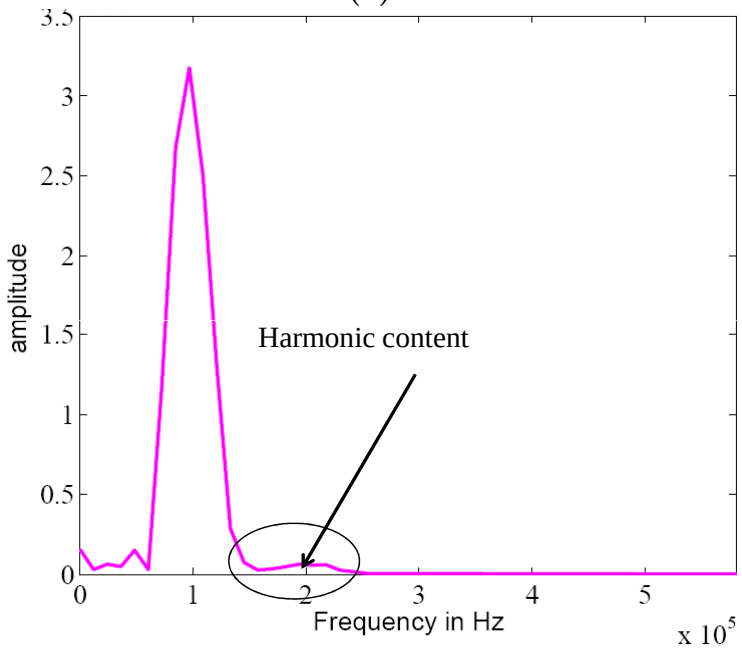

(b)

Figure 12: (a)Nonlinear bulk wave simulation(b) FFT obtained for nonlinear wave propagation simulation in 2D

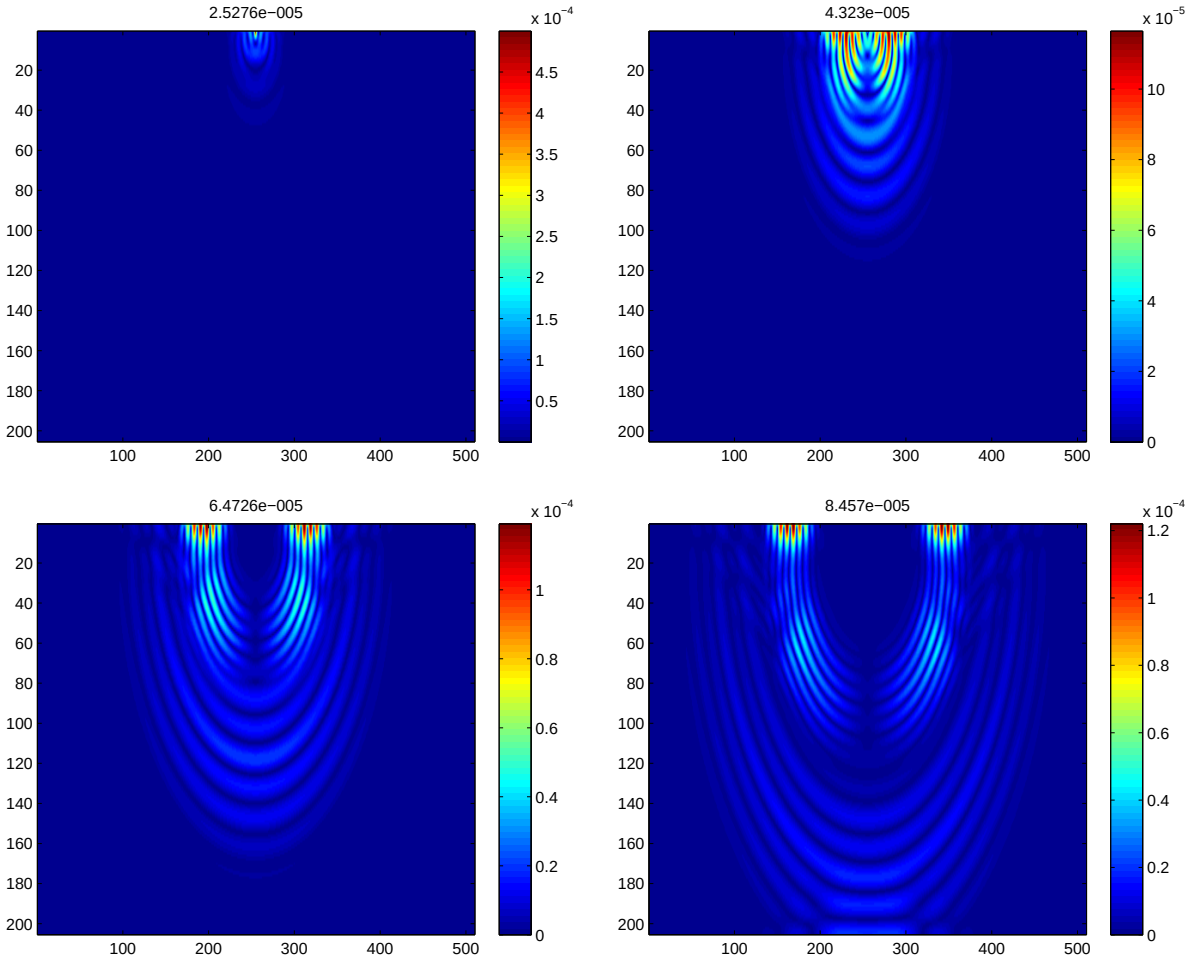

Figure 13: (a)Nonlinear rayleigh wave simulation obtained at different time periods

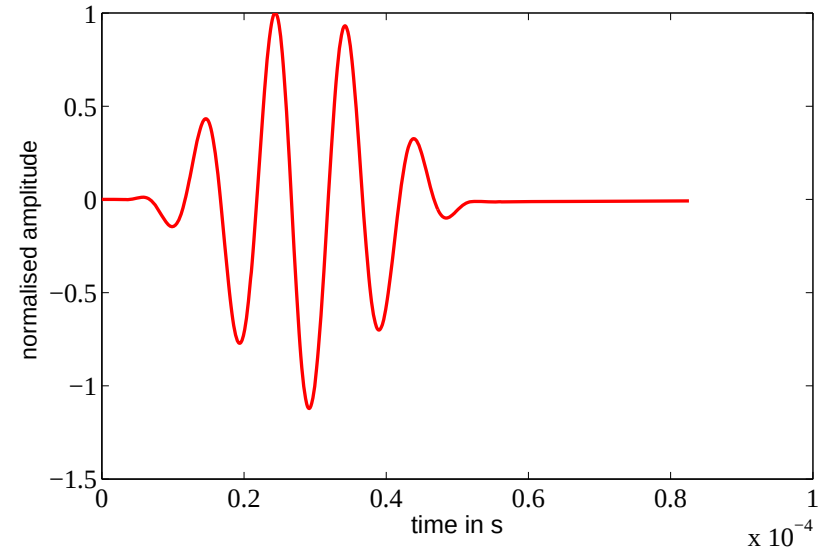

(a)

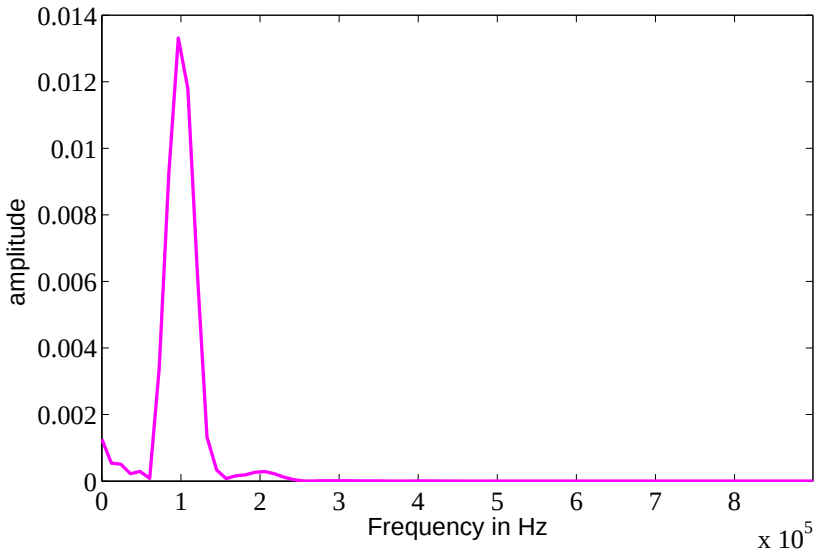

(b)

Figure 14: (a)Nonlinear Rayleigh wave signal(b) FFT obtained for nonlinear Rayleigh wave propagation simulation in 2D

APPENDIX B

Non-Linear Ultrasonic Experimental studies on Cu Alloys subjected to heat treatment.

Nonlinear ultrasonic method for the characterisation of microstructural changes associated with isothermal and isochronous annealing in pure copper

Abstract

In this study, sensitivity of nonlinear ultrasonic measurements towards annealing in polycrystalline pure copper is presented. It is well known that, annealing above the recrystallisation temperature results in grain growth and it in turn modifies mechanical properties. Microstructural changes associated with isothermal as well as isochronous annealing and its concurrent influence on nonlinearity parameter is elucidated. Further, micro-hardness measurements as well as metallographic studies are conducted to underscore the selection of nonlinear ultrasonic method for the characterisation of annealing.

Keywords: Annealing; nonlinear ultrasonics; recrystallisation; microstucture; grain growth

Mechanical integrity of structural components are heavily dependent on accumulated damage or degradation of material properties. Such microstructural aberrations include voids, dislocations, micro and macro cracks, inclusions, persistent slip bands etc. Presence of these nonlinearities will affect the in-service performance of components in one way or other. Hence it is essential to detect such microdamages of serving components at an early stage. However, widely used linear ultrasonic method, employing ultrasonic velocity and attenuation, is incapable for early damage detection. Even-though these small amplitude waves are sensitive to gross defects, it is insensitive to close contact defects. Numerous studies on nonlinear ultrasonic (NLU) method, which employs high amplitude ultrasonic waves, has proved that it is an efficient tool for microstructural characterisation. Recent studies have demonstrated the efficacy of NLU for the characterisation of material prop-

erty degradation due to fatigue damage [1–7], creep damage [8–11], thermal degradation [12, 13], radiation damage [14] etc.. Microstructural changes such as void formation, coalescence of voids to micro crack and its growth to macro crack, formation of veins and persistent slip bands, precipitation of second phase particles, substructure formation and others could effectively be detected with NLU method. It is noteworthy that, finite amplitude ultrasonic waves are employed in nonlinear ultrasonic method. Moreover, due to the nonlinear elastic properties of the material, strong nonlinear effects are produced. The distortion of pure sinusoidal waves and its manifestation in the form of harmonic generation is an indication of nonlinearity in the material. Nonlinearity parameter β is used to quantify the amount of distortion. The distortion of waves can be attributed to the anharmonicity of lattice or due to the presence of dislocations present in the material [15]. Thus NLU technique is found to be most suitable to study the influence of dislocation density, substructural changes, precipitates and micro cracks. Quantification of the nonlinearities in materials in terms of β has been reported by several research groups[3, 4, 10].

It is well known that, heat treatment processes such as annealing, tempering, hardening etc. drastically modifies the microstructural characteristics of metals. Microstructural changes accompanying these processes affect its nonlinearities. Effects of intermetallics, formed during ageing treatment in 2205 duplex stainless steel [13] and second phase particles formed during solution annealing and subsequent ageing in M250 grade maraging steel, on nonlinearity parameter β can be seen in[16]. Presence of precipitates increase the strength of material and it is desirable to some extend only, and the coarsening of precipitates due to over ageing will lead to property degradation. Li et al [17] used NLU method for the assessment of material condition in heat treated inconel X-750 alloy. Improvement of its material properties due to heat treatment results in a decrease in nonlinearity. The influence of nonlinearity parameter on precipitates formed during heat treatments in different alloys were considered so far. Nevertheless, not much attention had been paid to understand nonlinearities of pure material owing to the simple heat treatment processes. In this study we attempts to investigate the influence of nonlinearity parameter β on the microstructural changes associated with annealing in a pure material. For the present study, selected material is pure copper(Cu) and heat treatment is annealing.

During annealing, recovery, recrystallisation and grain growth occur. Here, isothermal annealing with varying holding time and isochronous annealing with different temperatures were considered separately. Isothermal annealing was done at 677^0C for different holding time. Isochronous annealing was done for 1 h at various temperatures from 300^0C to 800^0C with an interval of 100^0C. Samples for the study was taken from a copper strip which contains rolling texture and lot of dislocations. Such a deformed material undergoes recovery, recrystallisation and grain growth as a result of annealing [18]. Energy stored in the dislocations during deformation is released in the recovery stage. Microstructure and properties of the material are partially restored to its original values in the recovery stage as some of the dislocations are annihilated or rearranged. Various stages in the recovery are, entanglement of dislocations, cell formation, annihilation of dislocations within cells, subgrain formation and subgrain growth[19]. In the recrystallisation stage new equi-axed, strain free grains will form. At recrystallisation temperature, 50% of the material is filled with recrystallized grains. With progress of time these grains grow and fill the entire deformed or recovered microstructure. To this end, it is essential to investigate, how these evolution of microstructural changes influence NLU measurements.

An ultrasonic wave with finite amplitude and frequency f_0 will generate frequency contents $2f_0$, $3f_0$ etc. as it pass through a nonlinear material. Quantification of nonlinearity present in a material is carried out by measuring nonlinearity parameters which depends on the amplitude of the frequency components. The amplitude of second harmonic content A_2 is directly proportional to the square of the amplitude of fundamental frequency component A_1 for constant distance of wave propagation [20]. The coefficient of proportionality is the second order nonlinearity parameter β, which gives information about the anharmonicities in the inter atomic forces and also about the dynamics of dislocation motion[21]. It is the combination of second and third order elastic constants, C_{ij} and C_{ijkl}, and can be represented in terms of amplitudes of frequency components. Thus nonlinearity parameter can be depicted as $\beta = 8A_2/k^2xA_1{}^2$, where k is the wavenumber and x is the wave propagation distance.

Commercial pure copper with chemical composition, 99.9% Cu, 0.0125% Zn, 0.007% Pb, 0.0148% Sn, 0.0095% Ni, 0.0035% Ag, 0.0039% Al, 0.0031% S and 0.0147% O_2, was selected for this heat treatment studies. Thirteen sam-

ples were cut from copper strip with a final dimension 40mm x 30mm x 5.5mm. One sample was kept as reference sample and from the remaining samples, six were isothermally annealed at 677°C(950K) for varying holding times like 0.25 h, 0.5 h, 1 h, 2 h, 3 h and 5 h. Then, six samples were isochronously annealed for 1hr at 300°C, 400°C, 500°C, 600°C, 700°C and 800°C. Heat treatment was done in an inert atmosphere of argon to prevent oxidation. All samples were allowed to cool naturally inside the furnace. Heat treated samples were polished with emery paper for uniform surface finish and plane parallelness. The block diagram of the experimental set-up used for nonlinear ultrasonic measurement is shown in Fig. 1. Equipment used for nonlinear

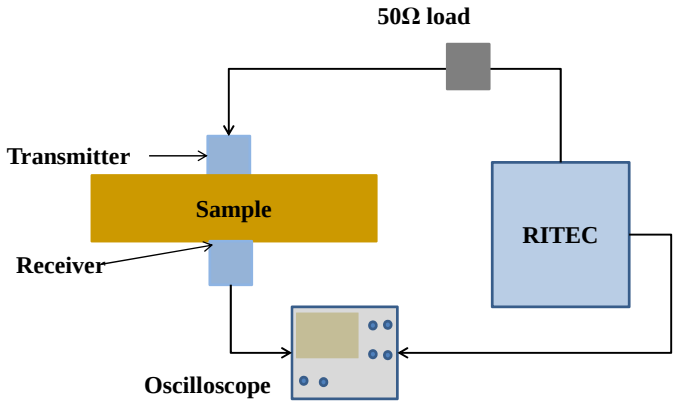

Figure 1: Block diagram of Nonlinear ultrasonic measurement set-up

ultrasonic study was RITEC RAM-5000 SNAP system. High power RF tone burst modulated with Hann window was send through a piezoelectric transducer of 5 MHz central frequency (Olympus NDT PANAMETRICS, V110) and 6mm element size. Another transducer with 10 MHz central frequency and of the same make and size, placed in through-transmission mode acts as the receiver. Proper contact between transducers and sample was ensured with a custom made fixture which could keep contact pressure constant. A uniform layer of couplant was provided by coconut oil. Number of cycles in the tone burst was limited to 8 to prevent the overlapping of multiple echoes. Output from the receiver was fed to AGILENT DSO 5012A oscilloscope, which could digitise the data at a sampling rate of 200 MHz. On each sample NLU measurement was taken at five positions and on each position, power level was varied from 40% to 90% of the maximum input power where the calibration curve was found as linear. Data corresponding to the time

domain signals was converted to frequency domain using an in-house program written in MATLAB. A time-domain signal obtained from nonlinear measurement and its corresponding fast Fourier transform (FFT) is given in Fig. 2. Using the amplitudes of fundamental frequency A_1 and second harmonic frequency A_2, second order nonlinearity parameter β is determined from the slope of the graph drawn with A_2 against $x{A_1}^2$. Thickness variation of samples due to polishing is also accounted.

The micro structure of Cu samples were determined using optical microscopy. Small specimens were cut from each heat treated sample using abrasive cutting machine and polished with different grades of emery paper. Final polishing was done with alumina. Polished samples were etched with a solution prepared from 1 g $K_2Cr_2O_7$, 4 ml H_2SO_4 and 50 ml H_2O. One drop of HCl was added just before use and the samples are swabbed with etchant for 15 seconds. Etched samples were viewed under a Leitz LABORLUX 12ME binocular optical microscope and metallographic images were analysed using METALPLUS software. Hardness of each heat treated sample was determined using Wolpert-Wilson microvickers hardness tester. Samples used for microhardness test were polished to optical finish and indentation was provided on each sample using a square pyramid indenter made out of diamond. For that, a load of 200 g was applied for a dwell period of 15 seconds. From the length of the diagonals of indentation, hardness value was determined.

Samples which were annealed at 677^0C underwent same recovery and recrystallisation stages. Due to the difference in holding time, grain growth differ in each sample. As annealing time increases, grain size also increases [22]. Variation of A_2 against the product of thickness x and square of A_1 for increasing power level is plotted in Fig. 3(a). A linear regression line can be fitted to correlate A_2 and A_1^2x with a correlation coefficient of 0.9976. Similar type of trend was seen for all heat treated samples. The slope of the trend line is proportional to nonlinearity parameter β. The behaviour of nonlinearity parameter β with holding time is plotted in Fig. 3(b). We noticed that, with increase in heat treatment time, nonlinearity parameter is decreasing and it reaches a minimum at 1 hour and thereafter it is showing an increasing trend. Nonlinearity is maximum for the untreated sample due to the high dislocation density and the texture formed due to prior rolling operation. Due to annealing, dislocations will annihilate or rearrange to a low energy state. Hence dislocation density will decrease and as a result of which nonlinearity parameter also decreases. Formation of new stress free,

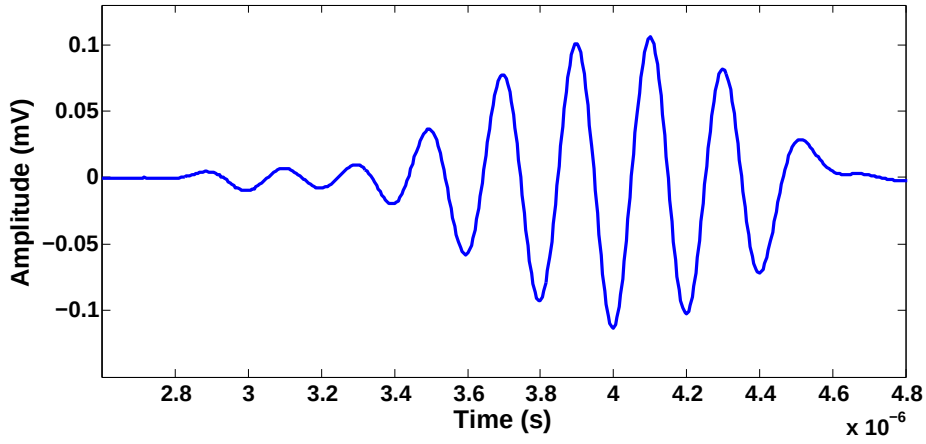

(a)

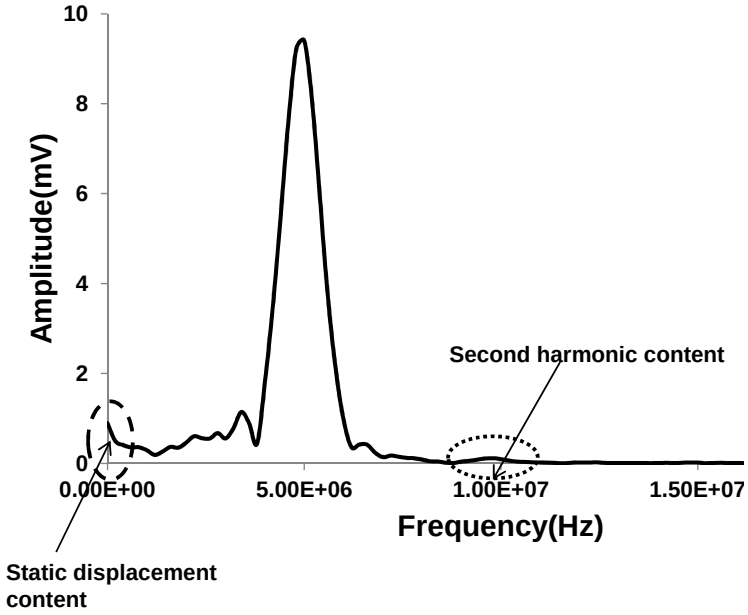

(b)

Figure 2: (a)Time domain signal obtained from nonlinear ultrasonic method(b)Fourier spectrum showing fundamental and harmonic components

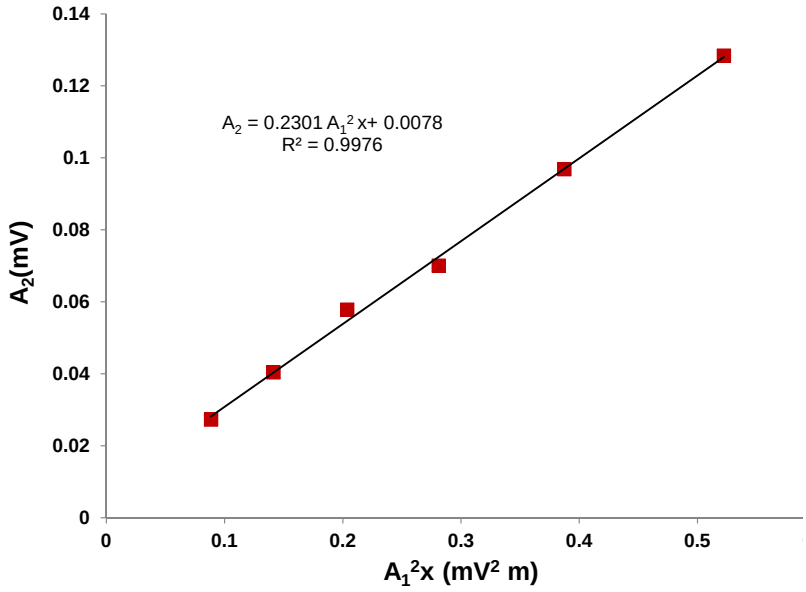

(a)

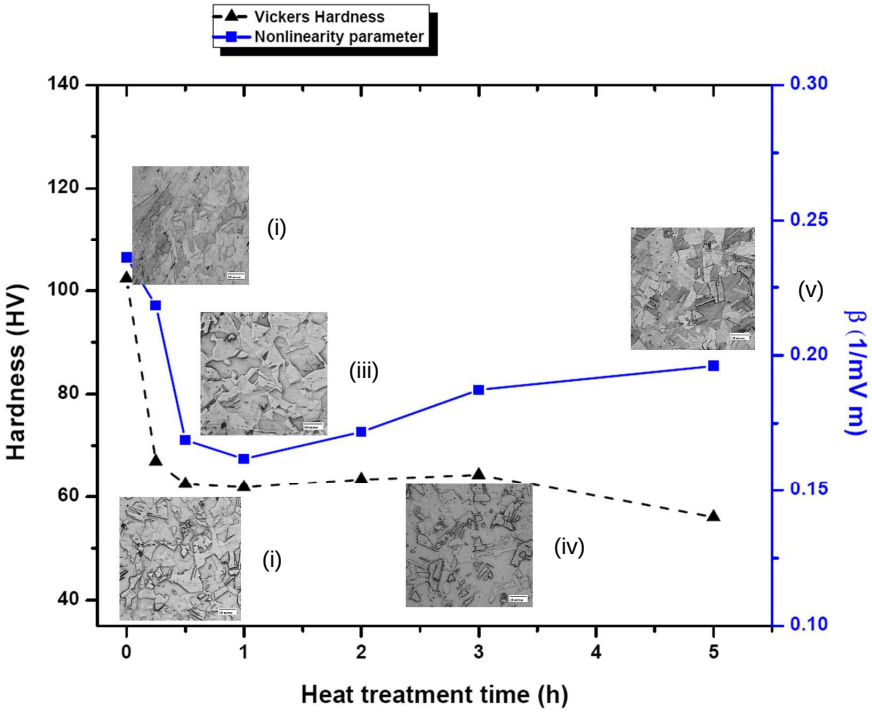

(b)

Figure 3: (a)A_2 vs A_1^2x for a heat treated sample(b)Behaviour of hardness value and nonlinearity parameter in isothermal annealing for (i) 0.25 h (ii) 0.5 h (iii) 1 h (iv) 3 h and (v) 5 h

equi-axed grains during recrystallisation also result in the reduction of nonlinearity parameter. From the micrograph included in Fig. 3, we found the presence of new grains as well as annealing twins. Minimum nonlinearity is observed for 1 hour annealing which result in grains of almost similar size. An increasing tendency for nonlinearity parameter is observed after 1 hour. Increment in nonlinearity parameter is due to abnormal grain growth and more annealing twins. Increase in grain size due to isothermal annealing, leads to a decrease in hardness. Average hardness value of as received sample is 102 HV. With increase in holding time, hardness decreases to a minimum of 62 HV corresponding to 1 hour heat treatment. Change in hardness value with heat treatment time is also depicted in Fig. 3.

In isochronous annealing samples were heat treated at different temperature by keeping the holding time constant. Isochronous annealing of samples result in an enhancement of grain size. With increase in grain size, nonlinearity parameter is showing a decreasing trend. Along with increase in grain size a decrease in hardness is observed in isochronous annealing. Variation of hardness and nonlinearity parameter with annealing temperature is shown in Fig. 4. Corresponding microstructural evolution is also included in the figure.

In this work nonlinear ultrasonic measurement has been performed to study the nonlinearities in pure copper due to annealing. Recovery, recrystallisation and grain growth are the stages in annealing. Isothermal annealing above the recrystallisation temperature of pure copper results in samples with same recovery and recrystallisation. Depending upon the holding time, grain growth as well as the amount of annealing twins will differ. Nonlinearity is maximum for as received sample due to the presence of large dislocations and texture. With annealing, nonlinearity is showing a decreasing trend. The decrease in nonlinearity is due to the presence of new strain free, equi-axed grains with less number of dislocations, formed as a result of recovery and recrystallisation. We noticed that, with increase in holding time, nonlinearity decreases and reaches a minimum value corresponding to 1 hour holding time and thereafter it is showing an increasing trend. One hour annealing time yields a microstructure with almost same grain size. Abnormal grain growth as well as the presence of more annealing twins results in a higher nnonlinearity after 1 hour holding time. Results of hardness measurement also showed a minimum hardness at 1 hour holding time and the trend is almost similar to the variation of nonlinearity with holding time. In the case of isochronous

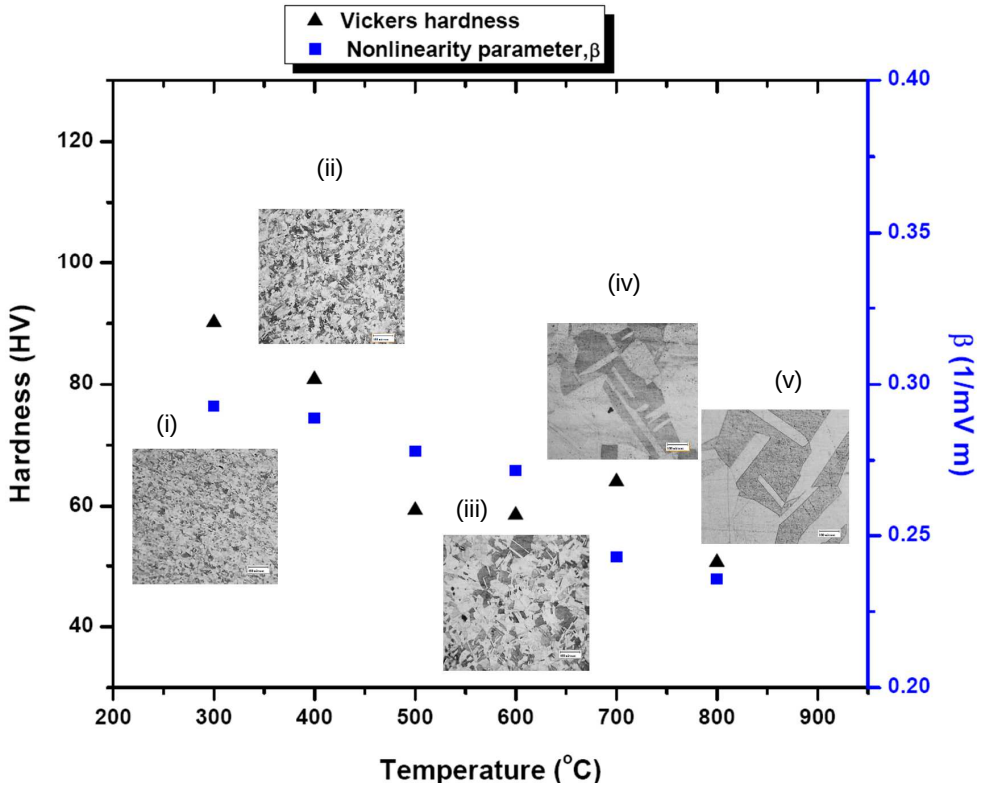

Figure 4: Behaviour of hardness value and nonlinearity parameter in isochronous annealing at (i) 300^0C (ii) 400^0C (iii) 600^0C (iv) 700^0C and (v) 800^0C

annealing, nonlinearity is showing a monotonous decrease. Hardness values and metallography images shows that with isochronous annealing grain size is increasing. Hence nonlinear ultrasonic method can be used for the characterisation of grain growth associated with annealing.

Authors gratefully acknowledges Prof. M.Kamaraj and Prof. M.Balasubramanian, Metallurgical and Material Engg., IIT Madras for providing research facilities for heat treatment and metallography studies. One of the author (R.S.Mini) also acknowledges the sponsorship provided by AICTE-QIP (Government of India).

References

[1] J. Frouin, S. Sathish, T. E. Matikas, J. K. Na, J. Mater. Res. 14 (1999) 1295–1298.

[2] J. Cantrell, W. Yost, Int. J. Fatigue 23 (2001) 487–490.

[3] J. Cantrell, J. Appl. Phys. 100 (2006) 063508.

[4] S. P. Sagar, S. Das, N. Parida, D. Bhattacharya, Scripta Mater. 55 (2006) 199 – 202.

[5] K. Ramkumar, R. Sivaramanivas, T. Karthik, V. Kommareddy, B. Ramadurai, B. Ganesan, E. Nieters, M. Gigliotti, M. Keller, M. Shyamsunder, Int. J. Fatigue 29 (2007) 2032–2039.

[6] A. Metya, N. Parida, D. Bhattacharya, N. Bandyopadhyay, S. Palit Sagar, Metall. Mater. Trans. A 38 A (2007) 3087–3092.

[7] W. Bin, Y. Bing-sheng, H. Cun-fu, T. Nonferr. Met. Soc. 21 (2011) 2597–2604.

[8] S. Baby, B. Nagaraja Kowmudi, C. Omprakash, D. Satyanarayana, K. Balasubramaniam, V. Kumar, Scripta Mater. 59 (2008) 818–821.

[9] J. S. Valluri, K. Balasubramaniam, R. V. Prakash, Acta Mater. 58 (2010) 2079 – 2090.

[10] K. Balasubramaniam, J. Valluri, R. Prakash, Mater. Charact. 62 (2011) 275–286.

[11] C. Kim, Mater. Trans. 53 (2012) 2028–2033.

[12] C. Kim, I.-K. Park, K.-Y. Jhang, NDT & E Int. 42 (2009) 204 – 209.

[13] A. Ruiz, N. Ortiz, A. Medina, J.-Y. Kim, L. Jacobs, NDT & Int. 54 (2013) 19–26.

[14] K. H. Matlack, J. J. Wall, J.-Y. Kim, J. Qu, L. J. Jacobs, H.-W. Viehrig, J. Appl. Phys. 111 (2012) 054911–13.

[15] M. A. Breazeale, J. Ford, J. Appl. Phys. 36 (1965) 3486–3490.

[16] A. Viswanath, B. Rao, S. Mahadevan, T. Jayakumar, B. Raj, J. Mater. Sci. 45 (2010) 6719–6726.

[17] W. Li, Y. Cho, J. Lee, J. Achenbach, Exp. Mech. 53 (2013) 775–781.

[18] P. R. Rios, F. Siciliano Jr, H. R. Z. Sandim, R. L. Plaut, A. F. Padilha, Mater. Res. 8 (2005) 225 – 238.

[19] F. Campbell, Elements of Metallurgy and Engineering Alloys, A S M International, Incorporated, 2008.

[20] H. Cantrell, Ultrasonic Nondestructive Evaluation: Engineering and Biological Material Characterization, Taylor & Francis, 2003.

[21] R. B. Thompson, O. Buck, D. O. Thompson, J. Acoust. Soc. Am. 59 (1976) 1087–1094.

[22] A. Rollett, F. Humphreys, M. Hatherly, Recrystallization and Related Annealing Phenomena, Elsevier, 2004.